Parameterization of Infrared Absorption in Midlatitude Cirrus Clouds

KENNETH SASSEN

Geophysical Institute, University of Alaska, Fairbanks, Fairbanks, Alaska

ZHIEN WANG

University of Maryland, Baltimore County, Baltimore, Maryland

C. M. R. PLATT*

Department of Atmospheric Science, Colorado State University, Fort Collins, Colorado

JENNIFER M. COMSTOCK

Pacific Northwest National Laboratory, Richland, Washington

(Manuscript received 27 March 2002, in final form 13 August 2002)

ABSTRACT

Employing a new approach based on combined Raman lidar and millimeter-wave radar measurements and a parameterization of the infrared absorption coefficient σ_a (km^{-1}) in terms of retrieved cloud microphysics, a statistical relation between σ_a and cirrus cloud temperature is derived. The relations $\sigma_a = 0.3949 + 5.3886 \times 10^{-3}T + 1.526 \times 10^{-5}T^2$ for ambient temperature T(°C) and $\sigma_a = 0.2896 + 3.409 \times 10^{-3}T_m$ for midcloud temperature T_m(°C) are found using a second-order polynomial fit. Comparison with two σ_a-versus-T_m relations obtained primarily from midlatitude cirrus using the combined lidar–infrared radiometer (LIRAD) approach reveals significant differences. However, it is shown that this reflects both the previous convention used in curve fitting (i.e., $\sigma_a \to 0$ at ~ -80°C) and the types of clouds included in the datasets. Without such constraints, convergence is found in the three independent remote sensing datasets within the range of conditions considered to be valid for cirrus (i.e., cloud visible optical depth less than $\sim$3.0 and T_m less than ~ -20°C). Hence, for completeness, reanalyzed parameterizations for a visible extinction coefficient σ_e-versus-T_m relation for midlatitude cirrus and a data sample involving cirrus that evolved into midlevel altostratus clouds with higher optical depths are also provided.

1. Introduction

Understanding the radiative effects of clouds on the earth–atmosphere system is of crucial importance to improving the accuracy of general circulation models (GCM) to predict our current climate and to better comprehend climate change issues (Stackhouse and Stephens 1991). The chief radiative properties of clouds are expressed in terms of their visible cloud optical depth τ and infrared absorption emittance ε. Although these parameters depend on cloud microphysical content by way of variations in particle phase, size, and shape, or as expressed in many models by mass content and effective particle size, it is ambient temperature that, to a large extent, governs radiative transfer because of the strength of the adiabatic process. Thus, temperature is a basic factor in the parameterization of cloud radiative properties, and relations describing these temperature dependencies can be used to help to validate model calculations.

One important element in this endeavor is related to the component of cirrus clouds inhabiting the upper troposphere (Liou 1986). The essential radiative properties of these ice clouds are that they are optically thin ($\tau < \sim$3.0) in the visible and are gray emitters ($\varepsilon < \sim$0.85) in the infrared (Platt et al. 1987; Sassen 2002). Nonetheless, cirrus clouds are globally widespread and are well positioned in the upper troposphere to modulate the fluxes of incoming shortwave and outgoing longwave radiation (Wylie et al. 1994). Because of this, uncertainties related to the manner in which their radiative properties are treated in GCMs have become an

* Additional affiliation: CSIRO Division of Atmospheric Research, Aspendale, Victoria, Australia.

Corresponding author address: Kenneth Sassen, Geophysical Institute, University of Alaska, Fairbanks, P.O. Box 757320, Fairbanks, AK 99775.
E-mail: ksassen@gi.alaska.edu

important issue. Stephens et al. (1990), for example, related the relevance of the radiative properties of clouds to climate feedback, and Lohmann and Roeckner (1995) used a GCM to illustrate how different cirrus cloud emissivity parameterizations could have a large impact on the predicted global climate and sensitivity to climate change.

The infrared absorption coefficient σ_a is a basic cloud property from which the radiative transfer of infrared flux through a cloud can be calculated. It is convenient and most accurate to measure the cloud vertical emittance, and thus absorption coefficient, in a narrow band of wavelengths in the atmospheric window region. This value can then be related to broadband flux emittance and various reflectance considerations through theoretical or experimental values of spectral variation and diffusivity calculations (e.g., Platt and Dilley 1981).

In this study, we concentrate on the parameterization of the temperature dependence of σ_a in the midinfrared (9.25–12.0 μm) window, which is the basic term in computing ε. That is, in terms of cloud height Z and physical depth ΔZ,

$$\varepsilon = 1 - \exp\left[-\int_0^{\Delta Z} \sigma_a(Z)\, dZ\right]. \quad (1)$$

Although scattering may also have an effect on cirrus cloud radiative transfer in the thermal infrared, particularly from satellites, cirrus clouds radiative forcing is mainly affected by cloud absorption (Fu et al. 1997).

Here we present results from an extensive remote sensing dataset based on combined Raman lidar and millimeter-wave radar measurements of cirrus and using a newly developed algorithm to infer cirrus cloud content (Wang and Sassen 2002a). Our results are compared with similar parameterizations developed from combined lidar and infrared radiometer (LIRAD) datasets from Platt and Harshvardhan (1988) and Sassen and Comstock (2001). Although the equations are significantly different, we show how they can be reconciled by addressing the numerical form of curve fitting and confining the datasets to proper cirrus clouds [as defined in Sassen (2002)].

2. The lidar–radar dataset

As described in detail in Wang and Sassen (2002b), the current parameterizations are based on about 1000 h of combined Raman lidar (0.355-μm channel) and millimeter-wave (8.7 mm) cloud radar data from cirrus clouds obtained between 1996 and 2000 at the Southern Great Plains Clouds (SGP) and Radiation Test Bed (CART) site in north-central Oklahoma. The method relies on combining the measurements of equivalent radar reflectivity factor Z_e and lidar visible extinction coefficient σ_e to estimate vertical profiles of cirrus cloud ice water content IWC and general effective size D_{ge} (Fu 1996). As shown by Ansmann et al. (1992) and discussed in Wang and Sassen (2002b), no major assumptions, such as specifying the backscatter-to-extinction ratio, are required to retrieve the cirrus cloud extinction coefficient with this Raman lidar method. Based on the treatment of the radiative properties of cirrus clouds developed by Fu (1996), σ_e can be parameterized as a function of IWC and D_{ge} as

$$\sigma_e = \mathrm{IWC}(a_0 + a_1/D_{ge}), \quad (2)$$

where a_0 and a_1 are constants at visible wavelengths, and D_{ge} is defined in terms of the ice crystal width D, length L, and concentration N by

$$D_{ge} = \frac{\int_{L_{min}}^{L_{max}} D^2 L N(L)\, dL}{\int_{L_{min}}^{L_{max}} \left(DL + \frac{\sqrt{3}}{4} D^2\right) N(L)\, dL}. \quad (3)$$

Mitchell (2002) has recently discussed the approaches and limitations of determining an effective size for populations of nonspherical particles in radiative transfer calculations: such terms are an artifice involved in computing the scattering and absorption coefficients in clouds as a function of wavelength, not a representation of the physical size of an actual ice crystal.

Using the same assumptions concerning the hexagonal column shape of ice crystals as in Fu (1996), and further assuming that the Rayleigh approximation is valid and the radar reflectivity of the ice crystals is equal to that of an equivalent volume solid ice sphere (Liao and Sassen 1994), water-equivalent Z_e can be parameterized approximately as

$$Z_e = C'(\mathrm{IWC}/\rho_i) D_{ge}^b, \quad (4)$$

where C' is the radar constant, b is a constant based on the use of a modified gamma size distribution, and $\rho_i = 0.92$ g cm^{-3} is the density of an ice particle (assumed to be solid).

Having retrieved vertical IWC and D_{ge} profiles according to this parameterization, we can then solve for the infrared absorption coefficient σ_a, which, according to Fu et al. (1998), can be expressed as

$$\sigma_a = \frac{\mathrm{IWC}}{D_{ge}}(b_0 + b_1 D_{ge} + b_2 D_{ge}^2 + b_3 D_{ge}^3), \quad (5)$$

where the coefficients b_n are taken from Table 1b of Fu et al. (1998) for the midinfrared window region.

Figure 1 provides the results of this analysis in terms of the dependence of σ_a on ambient temperature T in 1.0°C intervals. For this first result, we show the standard deviations for each data value, which indicate the considerable variability that exists in σ_a at all cloud temperatures. Frequency distributions of the σ_a at four selected temperatures (within 3.0°C temperature bins) are given in Fig. 2 to further illustrate this point. The distributions broaden with increasing temperature in a manner very similar to that reported for the visible ex-

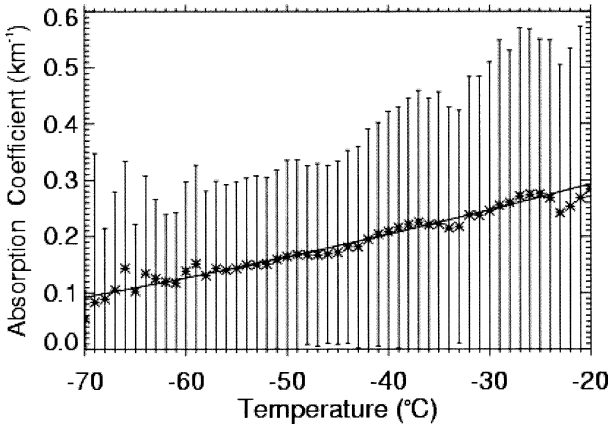

FIG. 1. Dependence of 1.0°C-average infrared absorption coefficients on *ambient* temperature derived from approximately 1000 h of combined Raman lidar and millimeter-wave radar data from the SGP CART site. Bars give the standard deviations for each point, and the solid curve shows the result of our parameterization.

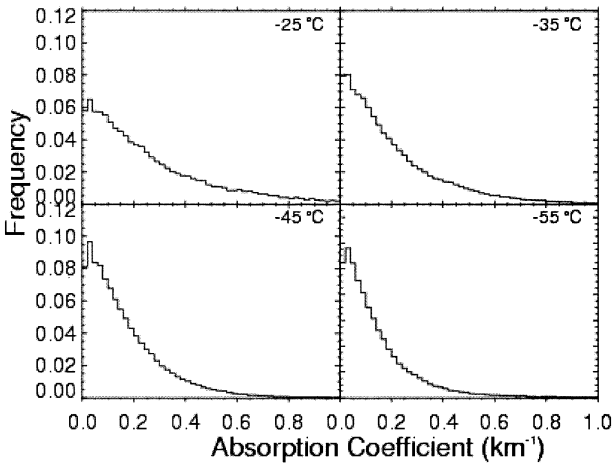

FIG. 2. Frequency distributions of the infrared absorption coefficient for four selected ambient temperatures, showing strong variability at any given temperature.

tinction coefficient in Wang and Sassen (2002b). A basic property of scattering and absorption in cirrus, then, is their strong variability even at a given temperature, which reflects the action of cloud microphysical process involving ice particle nucleation, growth, and vertical transport. Factors such as the cirrus cloud generating mechanism and the cloud-top temperature and relative position within the cloud (Sassen et al. 2002), also have impacts. As shown in Platt et al. (1987), the standard deviation of experimental uncertainties is typically much smaller than the natural variability of σ_a in clouds.

In Fig. 3, the dependence of σ_a on midcloud temperature T_m is shown, also in 1.0°C intervals. As in Fig. 1, the expected gradual decrease in average σ_a with decreasing temperature is clearly in evidence. Note that since both radar and lidar data are needed in the analysis, less accurate data occur at less than -65°C because of the bias in the radar measurements to sense only the densest cold cirrus (Wang and Sassen 2002b). In addition, anomalously high σ_a are found at the warmest T_m because this cloud sample appears to have included some relatively dense midlevel clouds (Sassen et al. 2001a; Sassen and Comstock 2001).

3. Current cirrus cloud σ_a parameterization

Using a second-order polynomial function to fit the extended datasets in Figs. 1 and 3, the results of our parameterizations of $\sigma_a(\text{km}^{-1})$ in terms of T and T_m (both in degrees Celsius) are shown by the solid lines in Figs. 1 and 3, respectively. The fitted equations are $\sigma_a = 0.3949 + 5.3886 \times 10^{-3}T + 1.526 \times 10^{-5}T^2$ and $\sigma_a = 0.2896 + 3.409 \times 10^{-3}T_m$.

4. Comparison with LIRAD parameterizations

The LIRAD method has been used previously to derive the relation between σ_a and T_m in primarily midlatitude cirrus clouds (Platt 1973; Platt and Dilley 1981; Comstock and Sassen 2001). (Note that, because this approach combines range-resolved lidar with path-integrated infrared radiometer measurements, it is only possible to provide information with respect to T_m.) With this method, simultaneous coaligned measurements of narrow-field-of-view infrared brightness temperature and lidar backscatter cross section are com-

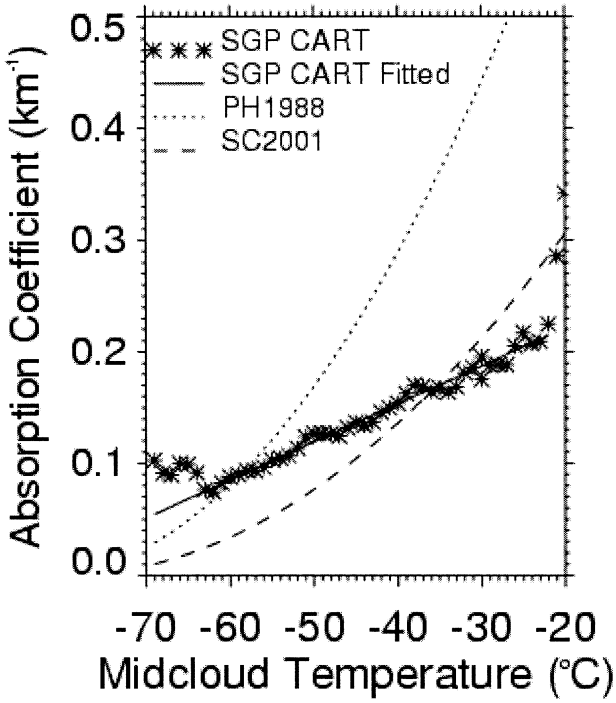

FIG. 3. Comparison of *midcloud* temperature vs absorption coefficient parameterizations from the current study (solid curve and 1.0°C-average σ_a), Platt and Harshvardhan (1988), and Sassen and Comstock (2001).

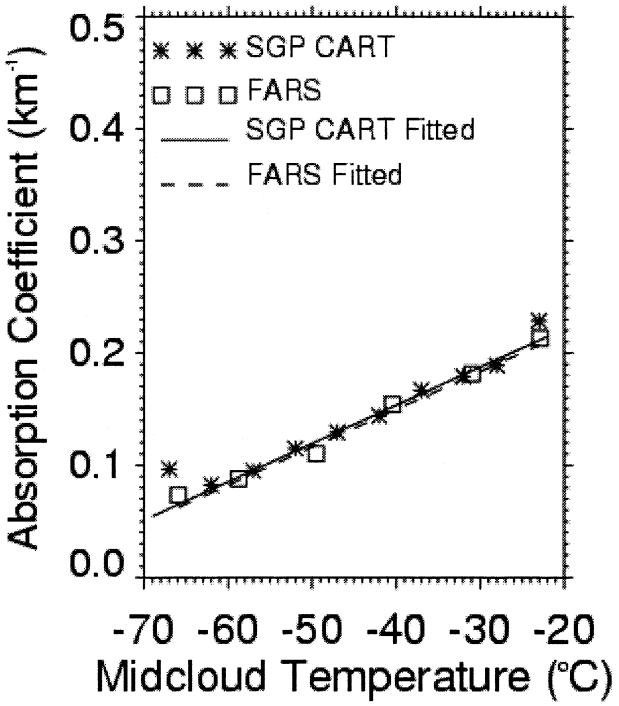

FIG. 4. Comparison of data points from the current study at the SGP CART and FARS sites for midlatitude cirrus clouds. Also shown are the new parameterized results for the two datasets.

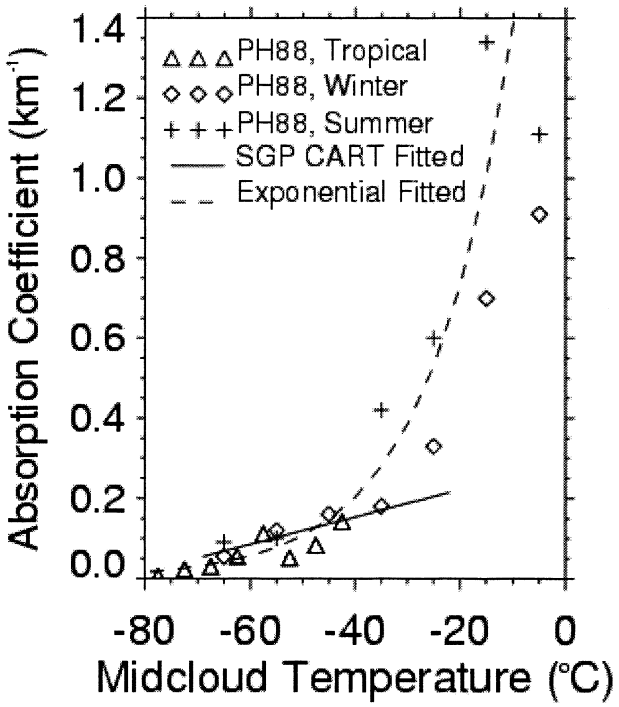

FIG. 5. Absorption coefficients from Platt and Dilley (1981) and Platt et al. (1987) plotted against midcloud temperature, as compared with the current SGP CART parameterization and a new exponential fit to the Southern Hemisphere data (dashed line) considered to be appropriate for high-level clouds that evolve into midlevel clouds.

bined to estimate τ and ε. The derived lidar cloud backscatter coefficient β_c, which is strongly dependent on the backscatter-to-extinction ratio k and multiple scattering parameter η, is related to σ_a by assuming $\sigma_a(z) = \zeta\beta_c(z)$. Final values of $\sigma_a(z)$ are obtained by iterating ζ and the combined parameter $k/2\eta$ until measured and model radiances agree. Cloud emittance is then calculated directly from $\sigma_a(z)$, and τ is calculated using the final value of $k/2\eta$ and integrating β_c between cloud base and top. The LIRAD method computes ε with an uncertainty of about 10% (Platt and Dilley 1981).

The LIRAD method, as described in Platt and Dilley (1981), provides values of ε and improved estimates of τ by assuming a single value of $k/2\eta$ for the entire cloud system, which is obtained from the integrated attenuated backscatter as ε tends to unity (Platt 1973). The ratio $k/2\eta$ can also be obtained for each individual lidar profile by comparing the average backscatter coefficient above the cloud to the expected molecular signal, as described Comstock and Sassen (2001). This method produces an uncertainty of about 24% in τ. The results given here from the University of Utah Facility for Atmospheric Remote Sensing (FARS; Sassen et al. 2001b) dataset are calculated using this new LIRAD approach.

Figure 3 compares the results of the parameterization from our radar–lidar analysis of cirrus clouds from the SGP CART site (solid line) with those from midlatitude and tropical cirrus in Australia [dotted line; from Platt and Harshvardhan (1988)] and the total cirrus cloud sample from the FARS site in northern Utah [dashed line; from Sassen and Comstock (2001)]. The FARS dataset has been restricted to only visually identified cirrus clouds. There are obviously significant differences in the σ_a-versus-T_m predictions offered by these cirrus cloud parameterizations.

5. Discussion

To help to evaluate the reasons for the differences in the curves in Fig. 3, we first provide, in Fig. 4, a comparison of the original data points composing the FARS and SGP CART datasets (see inserted key). Although the parameterized results are divergent, it can be seen that the data values are in very good agreement over the $-20°$ to $-70°$C midcloud temperatures appropriate for these midlatitude cirrus clouds (Sassen and Comstock 2001).

Similarly, Fig. 5 compares the individual data points from Platt and Harshvardhan (1988) to the lidar–radar-based parameterization (solid line) from the SGP CART site. In this case, data corresponding to $T_m < \sim -30$°C are in reasonable agreement with the SGP and FARS parameterizations, although at warmer temperatures the Southern Hemisphere data increase considerably faster.

Thus we conclude that the significant differences in the parameterized curves in Fig. 3 are primarily a result of the earlier convention used to fit the LIRAD datasets.

In addition, because of the inclusion of relatively warm cloud data in Platt and Harshvardhan (1988), which violates our working definition of cirrus clouds (Sassen 2002), this particular parameterization has also been affected during curve fitting by the relatively high σ_a values at the warmer temperatures. It is clear that if the use of a minimum cirrus cloud temperature (of ~ -80°C) for $\sigma_a = 0$ is avoided, then the two LIRAD-derived datasets appropriate for midlatitude cirrus clouds are in good correspondence with our current lidar–radar data based on a different approach. As a matter of fact, the dashed line in Fig. 4 represents the reanalysis of the FARS LIRAD dataset using a linear fit: the result is practically indistinguishable from the current curve.

It is of interest to note that the southern midlatitude LIRAD data from which the Platt and Harshvardhan (1988) parameterization was drawn included some cirrus cloud systems that evolved into deep altostratus clouds with greater optical depths. Such clouds at higher temperatures can be expected to contain larger ice crystals and their aggregates and thus to have higher absorption coefficients. This common evolution in cloud type, then, has been captured in this dataset and can be used to parameterize the development of high cloud systems into midlevel cloud systems. The dashed line in Fig. 5, which clearly curves away from the FARS and SGP results at warm temperatures, provides the following parameterization appropriate for these conditions: $\sigma_a = 2.6282 \exp(0.064T_m)$.

Last, note that the same concerns regarding minimum cirrus temperature constraints also apply to the parameterization of other cirrus cloud radiative properties such as τ or visible extinction coefficient σ_e, as was recently pointed out in Wang and Sassen (2002b). We therefore provide the following new parameterization of cirrus cloud σ_e versus T_m based on the extensive LIRAD data reported in Sassen and Comstock (2001): $\sigma_e = 0.49 + 0.0052T_m$. This equation is based on a linear curve fit but reflects the growth of cirrus clouds at temperatures < -80°C and produces results that are very similar to the second-order polynomial function developed in Wang and Sassen (2002b) using the same lidar–radar dataset as here.

6. Conclusions

The accurate parameterization of the visible extinction and infrared absorption coefficients versus cirrus cloud temperature is crucial for modeling the radiative effects of these upper-tropospheric clouds. Unfortunately, recent analyses of remote sensing datasets have generated significantly different relations.

However, we have been able to show that what appeared to be an inharmonious set of cirrus cloud σ_a-versus-T_m parameterizations is in effect mainly a consequence of the data curve fitting approach used in each case. The σ_a data derived previously from the LIRAD approach, which were stated to be valid over the range of observed temperatures, were assumed to go to zero at the frigid (i.e., for midlatitudes) temperature of about -80°C. Of course, the adiabatic process continues to produce ice mass at colder temperatures, as is especially clear in the occurrence of tropical cirrus clouds down to temperatures as cold as about -90°C (Sassen et al. 2000). Because of the drawbacks associated with minimum temperature constraints, we have provided a reanalyzed cirrus cloud σ_e-versus-T_m relationship based on extended LIRAD data from FARS.

It is also indicated that care must be taken to properly identify cloud type (e.g., cirrostratus versus altostratus) in the creation of parameterizations from extended measurements (Sassen 2002). In the case of the data from Platt and Dilley (1981) and Platt et al. (1987), the cloud sample included cirrostratus that developed into altostratus over the observation period. However, the Platt and Harshvardhan (1988) parameterization remains valid for these prefrontal cirrus/altostratus clouds observed at midlatitudes, and a new exponential σ_a-versus-T_m fit describing this common transition is offered here, with the following caveat. These clouds contained frequent layers of high backscatter and low depolarization (Platt et al. 1987), pointing to the presence of horizontally oriented ice crystals that could cause a larger emittance than for equivalent particles with random orientations using zenith lidar measurements.

We believe that additional research is needed to determine whether other types of cirrus clouds, particularly those derived from tropical deep convection, will need to be treated as distinct from the midlatitude cirrus considered here. Although the relatively small sample of tropical cirrus clouds from northern Australia in Platt et al. (1987) appears to be consistent with the midlatitude data presented in Fig. 5, because differences in radiative properties as a function of cirrus cloud generation mechanism have been identified in Sassen and Comstock (2001), it may prove useful for GCMs to stratify their treatment of cirrus clouds according to latitude or other factors. Recent observations of tropical clouds in Papua, New Guinea (Platt et al. 1998), for example, have indicated higher values of σ_a at the lower temperatures as compared with midlatitude clouds. We stress that the basic cirrus cloud generation process to a large extent controls the cloud microphysical conditions that ultimately determine their radiative properties.

Acknowledgments. This research has been funded by DOE Grant DEFG0394ER61747 from the Atmospheric Radiation Measurement Program and by NSF Grant ATM-0119502. Pacific Northwest National Laboratory is operated by Battelle for the U.S. Department of Energy.

REFERENCES

Ansmann, A., U. Wandinger, M. Riebesell, C. Weitkamp, and W. Michaelis, 1992: Independent measurement of extinction and

backscatter profiles in cirrus clouds by using a combined Raman elastic-backscatter lidar. *Appl. Opt.,* **31,** 7113–7131.

Comstock, J. M., and K. Sassen, 2001: Retrieval of cirrus cloud radiative and backscattering properties using combined lidar and infrared radiometer (LIRAD) measurements. *J. Atmos. Oceanic Technol.,* **18,** 1658–1673.

Fu, Q., 1996: An accurate parameterization of the solar radiative properties of cirrus clouds for climate research. *J. Climate,* **9,** 2058–2082.

——, K. N. Liou, M. C. Cribb, T. P. Charlock, and A. Grossman, 1997: Multiple scattering parameterization in thermal infrared transfer. *J. Atmos. Sci.,* **54,** 2799–2812.

——, Y. Ping, and W. B. Sun, 1998: An accurate parameterization of the infrared radiative properties of cirrus clouds for climate models. *J. Climate,* **11,** 2223–2237.

Liao, L., and K. Sassen, 1994: Investigation of relationships between K_a-band radar reflectivity and ice and liquid water contents. *Atmos. Res.,* **34,** 231–248.

Liou, K.-N., 1986: The influence of cirrus on weather and climate processes: A global perspective. *Mon. Wea. Rev.,* **114,** 1167–1199.

Lohmann, U., and E. Roeckner, 1995: Influence of cirrus cloud radiative forcing on climate and climate sensitivity in a general circulation model. *J. Geophys. Res.,* **100,** 16 305–16 323.

Mitchell, D. L., 2002: Effective diameter in radiative transfer: General definition, applications, and limitations. *J. Atmos. Sci.,* **59,** 2330–2346.

Platt, C. M. R., 1973: Lidar and radiometric observations of cirrus clouds. *J. Atmos. Sci.,* **30,** 1191–1204.

——, and A. C. Dilley, 1981: Remote sounding of high clouds. IV: Observed temperature variations in cirrus optical profiles. *J. Atmos. Sci.,* **38,** 1069–1082.

——, and Harshvardhan, 1988: Temperature dependence of cirrus extinction: Implications for climate feedback. *J. Geophys. Res.,* **93,** 11 051–11 058.

——, J. C. Scott, and A. C. Dilley, 1987: Remote sounding of high clouds. Part VI: Optical properties of midlatitude and tropical cirrus. *J. Atmos. Sci.,* **44,** 729–747.

——, S. A. Young, P. J. Manson, G. R. Patterson, S. C. Marsden, R. T. Austin, and J. H. Churnside, 1998: The optical properties of equatorial cirrus from observations in the ARM Pilot Radiation Observation Experiment. *J. Atmos. Sci.,* **55,** 1977–1996.

Sassen, K., 2002: Cirrus clouds: A modern perspective. *Cirrus,* D. Lynch et al., Eds., Oxford University Press, 11–40.

——, and J. M. Comstock, 2001: A midlatitude cirrus cloud climatology from the Facility for Atmospheric Remote Sensing. Part III: Radiative properties. *J. Atmos. Sci.,* **58,** 2113–2127.

——, R. P. Benson, and J. D. Spinhirne, 2000: Tropical cirrus cloud properties from TOGA/COARE airborne polarization lidar. *Geophys. Res. Lett.,* **27,** 673–676.

——, J. M. Comstock, and Z. Wang, 2001a: Parameterization of the radiative properties of midlatitude high and middle level clouds. *Geophys. Res. Lett.,* **28,** 729–732.

——, ——, ——, and G. G. Mace, 2001b: Cloud and aerosol research capabilities at FARS: The Facility for Atmospheric Remote Sensing. *Bull. Amer. Meteor. Soc.,* **82,** 1119–1138.

——, Z. Wang, V. I. Khvorostyanov, G. L. Stephens, and A. Benedetti, 2002: Cirrus cloud ice water content radar algorithm evaluation using an explicit cloud microphysical model. *J. Appl. Meteor.,* **41,** 620–628.

Stackhouse, P. W., and G. L. Stephens, 1991: A theoretical and observational study of the radiative properties of cirrus clouds: Results from FIRE 1986. *J. Atmos. Sci.,* **48,** 2044–2059.

Stephens, G. L., S. Tsay, P. W. Stackhouse Jr., and P. J. Flatau, 1990: The relevance of the microphysical and radiative properties of cirrus clouds to climate and climate feedback. *J. Atmos. Sci.,* **47,** 371–396.

Wang, Z., and K. Sassen, 2002a: Cirrus cloud microphysical property retrieval using lidar and radar measurements. Part I: Algorithm description and comparison with in situ data. *J. Appl. Meteor.,* **41,** 218–229.

——, and ——, 2002b: Cirrus cloud microphysical property retrieval using lidar and radar measurements. Part II: Midlatitude cirrus microphysical and radiative properties. *J. Atmos. Sci.,* **59,** 2291–2302.

Wylie, D. P., W. P. Menzel, H. M. Woolf, and K. I. Strabala, 1994: Four years of global cirrus cloud statistics using HIRS. *J. Climate,* **7,** 170–184.